

Generalization Properties of Stochastic Optimizers via Trajectory Analysis

Liam Hodgkinson
ICSI and Department of Statistics
University of California, Berkeley
`liam.hodgkinson@berkeley.edu`

Umut Şimşekli
INRIA - Département d’Informatique de l’École Normale Supérieure
PSL Research University
Paris, France
`umut.simsekli@inria.fr`

Rajiv Khanna
Department of Statistics
University of California, Berkeley
`rajivak@berkeley.edu`

Michael W. Mahoney
ICSI and Department of Statistics
University of California, Berkeley
`mmahoney@stat.berkeley.edu`

Abstract

Despite the ubiquitous use of stochastic optimization algorithms in machine learning, the precise impact of these algorithms on generalization performance in realistic non-convex settings is still poorly understood. In this paper, we provide an encompassing theoretical framework for investigating the generalization properties of stochastic optimizers, which is based on their dynamics. We first prove a generalization bound attributable to the optimizer dynamics in terms of the celebrated Fernique–Talagrand functional applied to the *trajectory* of the optimizer. This data- and algorithm-dependent bound is shown to be the sharpest possible in the absence of further assumptions. We then specialize this result by exploiting the Markovian structure of stochastic optimizers, deriving generalization bounds in terms of the (data-dependent) *transition kernels* associated with the optimization algorithms. In line with recent work that has revealed connections between generalization and heavy-tailed behavior in stochastic optimization, we link the generalization error to the *local tail behavior* of the transition kernels. We illustrate that the local power-law exponent of the kernel acts as an *effective dimension*, which decreases as the transitions become “less Gaussian.” We support our theory with empirical results from a variety of neural networks, and we show that both the Fernique–Talagrand functional and the local power-law exponent are predictive of generalization performance.

1 Introduction

Fundamental to the operation of modern machine learning is *stochastic optimization*: the process of minimizing an objective function via the simulation of random elements. Its practical ubiquity is matched by its theoretical depth; for decades, optimization theorists have sought to explain the surprising generalization ability of stochastic gradient descent (SGD) and its various extensions for non-convex problems — most recently in the context of neural networks and deep learning. Classical convex optimization-centric approaches fail to explain this phenomenon. Indeed, it is

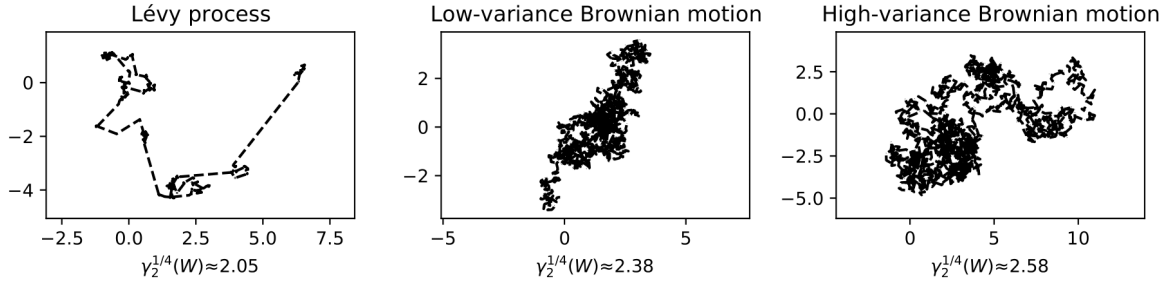


Figure 1: Discrete sample path approximations of a heavy-tailed α -stable Lévy process with $\alpha = 1.5$, and two Brownian motions with differing variances. Estimates of our normalized Fernique–Talagrand functional $\gamma_2^{1/4}(\cdot)$ is reported under each figure.

becoming increasingly clear that the performance of stochastic optimizers is largely dictated by their behavior in the highly stochastic initial phases of learning [34]. Consequently, it has become popular to take the variational approach of analyzing stochastic optimizers as dynamical systems [38, 50].

On the other hand, numerous efforts have been made to explain the success of deep learning by tying generalization performance to properties of the *loss landscape* [68]. Approaches that have received particular attention include those involving sharpness of minima; in particular, there is evidence that landing in “flat” optima often corresponds to improved generalization performance [17, 33]. As an alternative to these approaches, which depend on properties of the final trained model, our investigation centers around the following question: *Can generalization performance be explained through the dynamics of the optimizer seen in a single trajectory?* There is significant empirical evidence to suggest this could be the case [29–31, 42, 44, 66]. At the very least, important properties of the loss landscape should be reflected in the dynamics of the optimizer. For example, sharpness of minima dictates the size of the stochastic gradient, and hence the variance of fluctuations in SGD. Indeed, previous analyses have successfully tied variances of the optimizer to generalization [26, 47].

Our central motivation in this paper is the explicit inclusion of all information surrounding the dynamics of the optimizer as it applies to generalization performance. In particular, we may not necessarily be able to capture all the information by considering only generalization at any single point during (or at the end of) the optimization. Therefore, to answer our main question more generally, the quantity of interest in this work is an *accumulated generalization error* over the trajectory of the optimizer:

$$\sup_{t \in [t_1, t_2]} |\mathcal{R}_n(W_t) - \mathcal{R}(W_t)| = \sup_{w \in \{W_t\}_{t=t_1}^{t_2}} |\mathcal{R}_n(w) - \mathcal{R}(w)|, \quad (1)$$

where \mathcal{R} and \mathcal{R}_n denote the risk and empirical risk functions, respectively.

We shall note that if τ is an (early) stopping time dependent on an external validation set, and lies almost surely in $[t_1, t_2]$, then the generalization error at τ is bounded by (1). From this viewpoint, bounding (1) accounts for early stopping as well. Another advantage of considering (1) is that the presence of the supremum enables tools from analytic probability theory surrounding uniform error bounds. Therefore, to bound and estimate (1), we draw from this literature — in particular, a certain functional of Fernique [21] and Talagrand [61]. Applied to the trajectory of an optimizer, this Fernique–Talagrand functional simultaneously measures *variance* and *clustering* of the optimization trajectory (see Figure 1). Clustering in the optimization trajectory occurs in the absence of spatial homogeneity, and it can be measured in a number of ways.

Later, we will draw comparisons to Ripley’s K -function to make this connection more precise. In general, we will find that dynamics exhibiting lower variance and tighter clustering suggest better generalization performance.

1.1 Contributions

Our main contribution is a theoretical framework, which is comprised of two parts, that we develop for investigating the generalization properties of stochastic optimizers. In the first part, **(I)**, the generalization error attributable to optimizer dynamics is effectively reduced to a normalized *Fernique–Talagrand* (FT) functional. This functional is introduced in Section 2; and in Theorem 1, we obtain a sharp (up to constants) bound on the accumulated generalization error (1) in terms of our normalized FT functional applied to the trajectory of the optimizer, and the mutual information. In the second part, **(II)**, which is in Section 3, we proceed to bound the normalized FT functional, first in terms of Hausdorff dimension, recovering and extending the results of [59], and then in two original ways:

1. *Transition kernel:* Recalling that any practical stochastic optimization algorithm can be written as a Markov process [28], in Theorem 2, the expected normalized FT functional of the optimizer trajectory is bounded in terms of the transition kernel. Similar results are obtained for continuous-time Markov models as well. Our result illustrates effective dimension reduction through properties (e.g., variance) of the transition kernel.
2. *Local tail exponent:* Assuming that the optimizer displays random walk behavior in a neighborhood of the global optimum, in Corollary 2, we bound the expected normalized FT function in terms of a *local tail exponent*. This provides a discrete-time analogue to Corollary 1 and the work of [59], closing an open problem connecting generalization performance to power-law behavior in the dynamics of the optimizer.

Our contributions here are predominantly theoretical, motivated by recent work on state-of-the-art neural network models [42–44]. However, due to the relative tractability of estimating the FT functional and the local tail exponent, in Section 4, we demonstrate how these quantities could predict generalization performance in practice.

1.2 Related Work

For both motivation and comparison, we discuss some important previous efforts and adjacent concepts in the literature.

Generalization bounds. Naturally, there is a substantial literature involved in the development of “generalization bounds,” which we can only briefly summarize here. For more details, see [32] and references therein. Almost universally, these bounds consider “one-point generalization error,” that is $|\mathcal{R}_n(w) - \mathcal{R}(w)|$, for fixed weights w . Earlier bounds were typically dependent only on properties of the *model*, including Vapnik–Chervonenkis theory [64], and other norm-based bounds [6]. Most of these can be derived or sharpened through *generic chaining* [5], which we shall also reconsider, albeit for a different problem. Such bounds are well-known to be vacuous [7, 32, 43]. Non-vacuous bounds typically require some degree of *data-dependence*, with the most effective of these bounds involving measures of *sharpness* [32, 43, 49]. Other bounds also have some degree of *algorithm-dependence*, such as margin-based bounds [1, 60], or bounds centered around stochastic gradient Langevin dynamics [26, 47]. Specific to explaining the generalization in neural networks, which can even fit arbitrarily labeled data points [69], additional simplifying assumptions such as an infinite width [3], a kernelized approximation [11], or a simpler 2-layer setup [19] are usually made.

Mutual information. One particular class of generalization bounds involves the *mutual information* between the data and the stochastic optimizer, quantifying one-point generalization error by tying it to the learning ability of the algorithm itself [54, 67]. Intuitively, the mutual information balances the tradeoff between training loss and poor generalization due to overfitting. Such approaches are both data- and algorithm-dependent; and they can be made not only non-vacuous, but surprisingly tight [4]. Our Theorem 1 will also involve mutual information, extending [67] to bound the error (1). At present, applications of mutual information have tied variances in the optimizer to generalization [10, 26, 35, 48, 52]. Unfortunately, in larger models, the variance can anti-correlate with generalization [30, 43, 44], which, to our knowledge, these analyses are unable to predict.

Two phases of learning. It is clear that stochastic optimizers typically undergo at least two distinct phases of learning [36]: (1) an exploration-like “catapult” phase [34], when the step size is large, the optimizer moves rapidly between regions of the loss landscape, and more general patterns are fitted; and (2) an exploitation-like “lazy training” phase [12, 24], when the step size is small, dynamics behave similarly to convex optimization around a central basin, and more precise patterns are fitted. Performance in this second phase is easily tied to mixing rates using arguments from convex optimization theory. However, very little is known surrounding the first phase, despite its significant apparent influence on generalization performance. Here, we provide a theoretical framework enabling investigation into *both* of these phases.

Optimization-based generalization. A body of work leans on implicit regularization effects of optimization algorithms to explain generalization, e.g., see [2] and references within for certain simplified problem settings. Another line of work focuses on stability of the optimization process [27] to bound the generalization gap. These are also one-point generalization bounds, and they do not take into account the trajectory of optimization. In lieu of the inability of convex optimization theory to explain the behavior of SGD in non-convex settings, it is common to consider the behavior of Markov process models for stochastic optimizers [38]. These models are often continuous for ease of analysis [50, 58], although discrete-time treatments have become increasingly popular [16, 28]. Such continuous-time models are formulated as stochastic differential equations $dW_t = \mu(W_t)dt + \sigma(W_t)dX_t$, where X_t is typically Brownian motion, or some other Lévy process, and derived through the (generalized) central limit theorem and taking learning rates to zero [23].

Heavy-tailed universality. Recent investigations have identified the presence of heavy tails in the dynamics of stochastic optimizers [51, 57, 58]. Subsequent theoretical analyses trace the origins of these fluctuations to the presence of multiplicative noise [25, 28]. Establishing theory connecting generalization performance to the presence of power laws has become a prominent open problem in light of the empirical and theoretical studies of Martin and Mahoney [39–42, 44]; these studies have explicitly tied performance to the presence of heavier tails in the spectral distributions of weights. Of particular note is the previous work of [59], correlating generalization performance with heavier-tailed dynamics; this work considered (1) in the case $(t_1, t_2) = (0, 1)$ and in the context of continuous-time stochastic optimizer models. However, their approach is bound to a continuous-time Feller process model of the optimizer; and a significant objective of this work is to extend these ideas into the natural discrete-time setting.

2 Generalization and the Fernique–Talagrand functional

2.1 Background

Let $\ell : \mathbb{R}^D \times \mathbb{R}^p \rightarrow \mathbb{R}_+$ be a non-negative loss function assessing accuracy for a model with parameters $w \in \mathbb{R}^D$ to data $X \in \mathbb{R}^p$. For a collection of data $X_1, \dots, X_n \in \mathbb{R}^p$, each of which are assumed to be iid random variables, the empirical risk function is given by $\mathcal{R}_n(w) = n^{-1} \sum_{i=1}^n \ell(w, X_i)$. Therefore, letting $R_i(w) = \ell(w, X_i) - \mathbb{E}\ell(w, X)$, the error in the empirical risk is given by $n^{-1} \sum_{i=1}^n R_i(w)$. Our objective is to bound the maximal error in the empirical risk over some set $W \subset \mathbb{R}^D$. Assuming that ℓ is bounded in magnitude by $B > 0$, from McDiarmid’s inequality, with probability at least $1 - \delta$, it holds that

$$\max_{w \in W} |\mathcal{R}_n(w) - \mathcal{R}(w)| \leq \mathbb{E} \max_{w \in W} |\mathcal{R}_n(w) - \mathcal{R}(w)| + B \sqrt{\frac{\log(1/\delta)}{n}}.$$

In the case where W is finite, a naive union bound implies

$$\mathbb{E} \max_{w \in W} |\mathcal{R}_n(w) - \mathcal{R}(w)| \leq B \sqrt{\frac{\log(2|W|)}{2n}}, \quad (2)$$

which holds regardless of the properties or geometry of W . Up to constants, provided $\log(2|W|) = o(n)$, this is the best that one can achieve by assuming *only* that the loss is bounded (see [63, Theorem 5.3.3], for example).

To improve these bounds, it is common to assume that the loss functions are Lipschitz in w with respect to some metric on \mathbb{R}^D . In particular, for some metric $(x, y) \mapsto d(x, y)$ on \mathbb{R}^D , assuming that $|R_i(w) - R_i(w')| \leq Ld(w, w')$ for $w, w' \in W$, Hoeffding’s inequality implies that the difference in the error in the empirical risk between two points $w, w' \in W$ is subgaussian with variance parameter $(Ld(w, w'))^2$. Dudley’s classical method of chaining [18] asserts that one can take advantage of the triangle inequality to “chain” these bounds together over particular choices of w, w' and to bound the maximal error over the set W . Talagrand [61] later improved on this approach and developed *generic chaining*. This approach is heavily inspired by the following functional originally introduced by Fernique [21, 22]:

$$\gamma_2(W, d) = \inf_{\mu} \sup_{w \in W} \int_0^{\text{diam}(W)} \sqrt{\log \frac{1}{\mu(B_r^d(w))}} dr, \quad (3)$$

where $B_r^d(w) = \{w' : d(w, w') \leq r\}$ is the ball of radius r under d about w , $\text{diam}(W) = \sup_{w, w' \in W} d(w, w')$, and the infimum is taken over all probability measures μ supported on W . We refer to the functional (3) as the *Fernique–Talagrand (FT) functional*. Generic chaining would later focus on an (equivalent, up to constants) discrete variant of this functional [5, 62, 63], but for our purposes, we will find it more convenient to work with the original formulation (3).

Talagrand also showed that this approach is essentially *optimal* in the following sense: if the error $w \mapsto \mathcal{R}_n(w) - \mathcal{R}(w)$ is a Gaussian process with covariance $(w, w') \mapsto (Ld(w, w'))^2$, then the FT functional both upper and lower bounds the maximal expected error in the empirical risk $\mathbb{E} \sup_{w \in W} |\mathcal{R}_n(w) - \mathcal{R}(w)|$ up to constants [61, Theorem 5.1]. Therefore, in the absence of additional information on the distribution of the empirical risk, the FT functional provides the *sharpest possible generalization bound* up to constant factors.

2.1.1 Data-dependence with mutual information

In the classical theory, W is fixed deterministic. In the event that W is random but independent of the data X , by a conditioning argument, the same maximal expected error in the empirical

risk is bounded above and below by the *expected* FT functional, up to constants. However, in our setting of (1), W is both random and data-dependent. To extend the theory to allow for data-dependent W , we shall later invoke some ideas from information theory. Recall that the α -Renyi divergence is defined for $\alpha > 1$ by

$$D_\alpha(\mu, \nu) = \frac{1}{\alpha - 1} \log \mathbb{E} \exp \left(\alpha \log \frac{d\mu}{d\lambda}(Z) + (1 - \alpha) \log \frac{d\nu}{d\lambda}(Z) \right),$$

where Z is distributed according to some probability measure λ where μ and ν are absolutely continuous with respect to λ (for example, $\lambda = \frac{1}{2}(\mu + \nu)$). The α -mutual information between two random elements X, Y is defined as the α -Renyi divergence between the joint probability measure $\mathbb{P}_{X,Y}$ and the product measure $\mathbb{P}_X \otimes \mathbb{P}_Y$:

$$I_\alpha(X, Y) = D_\alpha(\mathbb{P}_{X,Y} \| \mathbb{P}_X \otimes \mathbb{P}_Y).$$

In essence, the α -mutual information measures the extent of the dependence between X and Y . The standard Kullback-Leibler mutual information is obtained by taking $\alpha \rightarrow 1^+$. The α -mutual information is non-decreasing in α , that is, $I_\alpha(X, Y) \leq I_\beta(X, Y)$ for $\alpha \leq \beta$. Therefore, we may define the total mutual information as $I_\infty(X, Y) = \lim_{\alpha \rightarrow \infty} I_\alpha(X, Y) = \sup_\alpha I_\alpha(X, Y)$.

2.1.2 Markov stochastic optimizers

In line with (1), we will typically take W to be the trajectory of a stochastic optimizer. To model this trajectory, we invoke the Markov formulation of stochastic optimizers, seen in [28]; this formulation incorporates SGD, momentum, Adam, and stochastic Newton, among others. To summarize, approximate solutions to problems of the form $\arg \min_w \mathbb{E} \ell(w, X)$ are typically obtained by fixed point iteration: for some continuous map Ψ such that any fixed point of $\mathbb{E} \Psi(\cdot, X)$ is a minimizer of ℓ , a stochastic optimizer is constructed from the sequence of iterations $W_{k+1} = \Psi(W_k, X_k)$, where X_k are independent copies of X . For example, stochastic gradient descent corresponds to the choice $\Psi(w, x) = w - \gamma b^{-1} \sum_{i=1}^b \nabla \ell(w, x_i)$, where γ is a chosen learning rate and b denotes the batch size. These iterations induce a discrete-time Markov chain in W_k with transition kernel $P(w, E) = \mathbb{P}(W_{k+1} \in E | W_k = w)$. Under certain regimes (for example, small learning rate and large batch size), this chain is well-approximated by a continuous-time Markov process $\{W_t\}_{t \geq 0}$ with transition kernel $P_t(w, E) = \mathbb{P}(W_t \in E | W_0 = w)$ — see [23], for example.

2.2 Using the normalized Fernique–Talagrand functional

An important takeaway from the existence of the FT functional is the correspondence between the amount of information contained in the specific Lipschitz assumption considered and the sharpness of the bound. From [61, Theorem 5.1], the best generalization bounds one could hope to achieve by assuming only Lipschitz continuity of ℓ with respect to some metric d would arise (up to constants) from the FT functional (3). For example, if ℓ is not assumed to be bounded, but is assumed to be Lipschitz continuous with respect to the Euclidean metric, then the best bounds involve the FT functional with d the Euclidean metric. On the other hand, if W is finite and ℓ is assumed only to be bounded, then the FT functional with the discrete metric $d(x, y) = \mathbb{1}\{x \neq y\}$ coincides with the naive bound (2), which is also optimal.

It is often the case with generalization bounds that ℓ is assumed to be both bounded and Lipschitz-continuous with respect to the Euclidean metric. In this case, we find that the appropriate object is the following *normalized Fernique–Talagrand functional*: for any $\rho > 0$,

$$\gamma_2^\rho(W) = \inf_\mu \sup_{w \in W} \frac{1}{\rho} \int_0^\rho \sqrt{\log \frac{1}{\mu(B_r(w))}} dr, \quad (4)$$

where $B_r(w)$ denotes the Euclidean ball of radius $r > 0$ about w , and the infimum is once again over all probability measures μ on W . This corresponds to the choice of metric $d_\rho(x, y) = \min\{\rho, \|x - y\|\}$, where $\|\cdot\|$ is the usual Euclidean norm. Here, ρ is arbitrary, but we will often find it convenient for it to be one. Notice that the integrand is necessarily zero whenever $r > \text{diam}(W)$, so the upper limit can equivalently be taken to be $\min\{\rho, \text{diam}(W)\}$. The functional is considered normalized as it does not grow as $\text{diam}(W) \rightarrow \infty$.

Our main result for this section is presented in Theorem 1 below. If W is uncountable, we interpret probabilities and expectations of suprema over uncountable sets as the corresponding supremum over all possible countable subsets.

Theorem 1. *Assume that ℓ is bounded by $B > 0$ and L -Lipschitz continuous (with respect to the Euclidean metric). There exists a universal constant $K_1 > 0$ such that for any (random) closed set $W \subset \mathbb{R}^D$, with probability at least $1 - \delta$, for any $\rho > 0$,*

$$\sup_{w \in W} |\mathcal{R}_n(w) - \mathcal{R}(w)| \leq K_1 \max\{B, L\rho\} \left(\frac{\gamma_2^\rho(W)}{\sqrt{n}} + \sqrt{\frac{\log(1/\delta) + I_\infty(X, W)}{n}} \right). \quad (5)$$

Furthermore, there exists another universal constant $K_2 > 0$ such that

$$\mathbb{E} \sup_{w \in W} |\mathcal{R}_n(w) - \mathcal{R}(w)| \leq K_2 \max\{B, L\rho\} \left(\frac{\mathbb{E}\gamma_2^\rho(W) + \sqrt{I_1(X, W)}}{\sqrt{n}} \right). \quad (6)$$

Remark 1. The naive bound can also be readily recovered from $\gamma_2^\rho(W)$. Indeed, by letting $\mu(\{w\}) = 1/|W|$ for each $w \in W$, one can see that $\sqrt{-\log \mu(B_r(w))} \leq \sqrt{\log |W|}$ for all $r > 0$ and $w \in W$, and so $\gamma_2^\rho(W) \leq \sqrt{\log |W|}$. Since this holds uniformly in ρ , one can take $\rho \rightarrow 0^+$, so the bound is no longer dependent on L , whence the naive bound is recovered.

Note also that when $W = \{w^*\}$, where w^* is the location of the optimizer at some *deterministic* stopping time, we recover (up to constants) the information-theoretic bound of [67]. Therefore, we inherit the interpretation of mutual information as a measurement of “overfitting,” together with its follow-up developments [4, 26]. The advantage of our bound is that we can better investigate the effect of dynamics on generalization through the supremum over the trajectory. We also inherit the sharpness of Theorem 1 from that of the FT functional in the event that X and W are independent.

Our remaining theoretical contributions are concerned with bounding and estimating γ_2^ρ when applied to the trajectory of a stochastic optimizer.

3 Bounding the Fernique–Talagrand functional

3.1 Fractal dimensions

It has been observed in [59] that the *fractal dimension* of the set W is often a good indicator of generalization performance. While this previous approach focused on precise covering arguments, here we show that a similar bound to [59, Theorem 2] can be readily attained using Theorem 1 under weaker assumptions. Indeed, Theorem 1 provides a remarkably straightforward illustration of the relationship between generalization performance and fractal dimension. Assuming there exists a measure μ on W such that $\mu(B_r(w)) \geq (cr)^\alpha$ for any $w \in W$ and $0 < r < \rho$, for some $c > 0$, $\alpha > 0$, then inserting this measure into the definition (4) reveals $\gamma_2^\rho(W) = \mathcal{O}(\sqrt{\alpha})$. If a similar upper bound also holds for μ , then most notions of fractal dimension of the set W coincide, and are precisely α [45, Chapter 5]. In this way, α becomes an *effective dimension*, or *intrinsic dimension*, of W (in particular, if $W \subset \mathbb{R}^D$, then $\alpha \leq D$, the ambient dimension). This

idea is formalized in Corollary 1, involving the *Hausdorff dimension* (for precise details on its definition, see Appendix A),

and improves on [59, Theorem 2]. To see this, note the assumption that $C_\rho > 0$ is contained in [59, H4], and arises in [59, Theorem 2] through the $\log n$ term, taking n sufficiently large.

Corollary 1. *Suppose that W has Hausdorff dimension α and is α -Ahlfors lower regular almost surely, that is,*

$$C_\rho^\alpha := \inf_{0 < r < \rho, w \in W} \frac{\mathcal{H}^\alpha(W \cap B_r(w))}{r^\alpha \mathcal{H}^\alpha(W)} > 0.$$

Then the normalized Fernique–Talagrand functional satisfies $\gamma_2^\rho(W) \leq (2\rho C_\rho)^{-1} \sqrt{\pi\alpha}$ almost surely.

A precise link to stochastic optimization comes through the following observation: suppose that W_t , $t \in [0, 1]$, is a continuous-time Markov process with transition kernel $P_t(x, E)$, e.g., a continuous-time model of a stochastic optimizer [50]. Combining [65, Theorem 4.1] and [45, Theorem 5.7], if W_t is spatially homogeneous, and

$$\alpha = \sup \left\{ \gamma \geq 0 : \lim_{r \rightarrow 0^+} r^{-\gamma} \int_0^1 P_t(0, B_r(0)) dt < +\infty \right\} \quad (7)$$

is defined and strictly positive, then $\{W_t\}_{t \in [0, 1]}$ is α -Ahlfors-regular almost surely, and hence Corollary 1 applies. Similar results also apply for spatially inhomogeneous Feller processes [55, 59]. Therefore, in the same vein as [59], Corollary 1 supports the claim that the fractal dimension of the image of a continuous Markov process can be an effective measure of exploration performance.

3.2 Sample paths of stochastic optimization algorithms as Markov processes

In reality, optimization procedures are not continuous-time and optimizer trajectories are finite sets. Since all fractal dimensions are identically zero on finite sets, an alternative approach is required. For this, we adopt the Markov model for stochastic optimizers. Fortunately, the FT functional is sufficiently versatile that we can provide a direct generalization bound in terms of transition kernels, without appealing to fractal dimensions. This is accomplished using more traditional covering arguments and the classical Dudley entropy bound [9, Corollary 13.2]. Here is our main result for this.

Theorem 2. *There exists a universal constant $K > 0$ such that the following bounds on the Fernique–Talagrand functional hold:*

1. *Let W_k , $k \geq 0$ be a discrete-time homogeneous Markov chain on \mathbb{R}^D with transition kernel $P^k(w, E)$. Then*

$$\mathbb{E} \gamma_2^\rho(\{W_k\}_{k=0}^m) \leq \frac{K}{\rho} \int_0^\rho \sqrt{(D+2) \log 3 - \inf_{x \in \mathbb{R}^D} \log \left(\frac{1}{m} \sum_{k=1}^m P^k(x, B_r(x)) \right)} dr.$$

2. *Let $\{W_t\}_{t \in [0, T]}$ be a continuous-time homogeneous Markov process on \mathbb{R}^D with transition kernel $P_t(w, E)$. Then*

$$\mathbb{E} \gamma_2^\rho(\{W_t\}_{t \in [0, T]}) \leq \frac{K}{\rho} \int_0^\rho \sqrt{(D+2) \log 3 - \inf_{x \in \mathbb{R}^D} \log \left(\frac{1}{T} \int_0^T P_t(x, B_r(x)) dt \right)} dr.$$

We can use Theorems 1 and 2 to bound the generalization error for a stochastic process as long as we can characterize the transition probability kernel of the process. Unlike Theorem 1, which we expect to be quantitatively non-vacuous, it is the qualitative interpretation in Theorem 2 that is significant. Following the logic of the previous section, the form of these bounds makes explicit how properties of the transition kernel reduce the effective dimension relative to the ambient dimension D . In particular, higher probabilities of smaller transitions suggest improved generalization performance.

3.3 Local homogeneity and tail behavior

While Theorem 2 successfully relates the dynamics of a Markov stochastic optimizer to generalization performance, the bound is ineffective when the increments $W_{k+1} - W_k$ are not universally stochastically bounded. This is the case in models of stochastic gradient optimizers when $\|\nabla f(x)\|$ is unbounded, which would certainly be true in the presence of L^2 regularization. Indeed, the bound in Theorem 2 is most tight when the optimizer exhibits random walk behavior without drift. This behavior is unlikely to occur at the global scale. However, *locally*, in the neighborhood of an optimum where $\|\nabla f(x)\|$ is small, a stochastic optimizer should exhibit minimal drift. Furthermore, in practice, the behavior around an optimum is typically of greatest interest.

Therefore, to address this deficiency, we appeal to approximation in total variation d_{TV} . Recall that the first objective of a stochastic optimizer is to reach and then occupy some central region Ω around a collection of optima $x^* \in \Omega$ with high probability. Within this region, we assume that the optimizer behaves closely to a random walk $\bar{W}_{k+1} = \bar{W}_k + Z_k$, where each Z_1, \dots, Z_k is independent and identically distributed. Furthermore, to develop a discrete time analogue of Corollary 1 (closing an open problem connecting tail exponents to generalization), we measure the clustering of this process through a power law exponent in the growth of the distribution function of Z_i . In particular, drawing inspiration from (7), our exponent α is defined such that the transition kernel $P(x, B_r(x)) \approx cr^\alpha$ as $r \rightarrow 0^+$. Note that, *a priori*, this is *distinct from the tail exponent* of the distribution considered in [28, 58, 59], although the two appear to correlate in practice (see Appendix C).

Corollary 2. *Let $\Omega \subseteq \mathbb{R}^D$ be a closed set such that $\mathbb{P}(W_k \notin \Omega \text{ for some } k = 0, \dots, m) \leq \zeta_m$. Suppose that $Z_1, \dots, Z_m \stackrel{iid}{\sim} \mu$ and there exists $r_0, \alpha > 0$ such that $\mathbb{P}(\|Z_1 + \dots + Z_k\| \leq r) \geq c_k r^\alpha$ for all $0 < r < r_0$, where $c_k > 0$ are constants for each $k = 1, 2, \dots$. Letting P_Ω denote the transition kernel of W_k conditioned on $W_k \in \Omega$ for $k = 1, 2, \dots, m$, there is a constant $K > 0$ such that for any $\epsilon > 0$, there exists $\rho_\epsilon > 0$ independent of α where*

$$\mathbb{E}\gamma_2^{\rho_\epsilon}(\{W_k\}_{k=0}^m) \leq \frac{K}{\rho_\epsilon} \sqrt{\alpha + \epsilon} + \sqrt{\log(m+1)} \left(\zeta_m + m \sup_{x \in \Omega} d_{TV}(P_\Omega(x, x + \cdot), \mu) \right). \quad (8)$$

Observe that for a random variable Z , $\mathbb{P}(Z \leq r) = \Omega(r^\alpha)$ as $r \rightarrow 0^+$ if and only if $\mathbb{P}(Z^{-1} > r) = \mathcal{O}(r^{-\alpha})$ as $r \rightarrow \infty$. Therefore, combining Corollary 2 with Theorem 1, the following conclusion is reached: for a stochastic optimizer exhibiting random walk behavior (oscillating about some central optima) in some interval $[t_1, t_2]$, an upper bound on the generalization performance in this interval is correlated to the tail exponent of the distribution of $\{\|W_{t+1} - W_t\|^{-1}\}_{t=t_1}^{t_2-1}$.

Arguably the most commonly considered discrete-time model for a stochastic optimizer is the perturbed gradient descent (GD) model, which satisfies $W_{k+1} = W_k - \gamma(\nabla f(W_k) + Z_k)$, where Z_k is a Gaussian random vector with zero mean and constant covariance matrix Σ representing noise in the stochastic gradient. In the neighborhood of a local optimum w^* , $\nabla f(W_k) \approx 0$, and

hence the perturbed GD model resembles a Gaussian random walk $W_{k+1} = W_k + \gamma Z_k$. Here, the exponent α is *precisely* the ambient dimension D (see Appendix B).

However, we will find this exponent to be much less than the ambient dimension for an actual optimization path, suggesting an interpretation of α as a measure of *effective dimension* for the purposes of generalization.

3.4 Variance and clustering

Now that two generalization bounds in Theorem 2 and Corollary 2 have been obtained involving the dynamics of the stochastic optimizer, we shall briefly discuss how two properties of the trajectory — variance and clustering — play a critical role in the Fernique–Talagrand functional.

First, we discuss the influence of “variance,” or the average size of fluctuations of the stochastic optimizer. Drawing from Theorem 2, we consider a continuous-time stochastic optimization model in the form of a stochastic differential equation $dW_t = \mu(W_t)dt + \sigma(W_t)dB_t$, where μ typically involves the gradient of the empirical risk \mathcal{R}_n . We assume that μ, σ are bounded with bounded second derivatives, and $\sigma(x)$ has non-zero singular values for all $x \in \mathbb{R}^D$. The Aronson estimates [56] imply that for some constant $K > 0$ and “minimal variance” $\lambda > 0$, $P_t(x, E) \geq Kt^{-D/2} \int_E \exp(-\|x - y\|^2/(2\lambda t)) dy$. This, together with Theorem 2, implies the existence of constants $K_1, K_2 > 0$ independent of T, λ such that (see Appendix B)

$$\mathbb{E}\gamma_2^\rho(\{W_t\}_{t \in [0, T]}) \leq \frac{K_1}{\rho} \int_0^\rho \sqrt{K_2 - D \log r - \log J_{\rho, T}(\frac{1}{2\lambda}, D)} dr, \quad (9)$$

where $J_{\rho, T}(a, D) = \frac{1}{T} \int_0^1 \int_{1/T}^\infty v^{D/2-1} s^{D/2-2} e^{-asv\rho^2} ds dv$ is monotone decreasing in a, D . It is important to note that λ will generally increase with the magnitude of μ, σ , and hence with the size of the stochastic gradient. Therefore, the normalized FT functional should increase monotonically with the variance of the fluctuations of the optimizer. Consequently, the *sharpness* of an optimum should be reflected in γ_2^ρ : in a “flat” neighborhood, the variance of fluctuations in the optimizer is small, and hence γ_2^ρ will be smaller.

Now, we move on to discuss how the α parameter in Corollary 2 can be interpreted as a measure of “clustering” of the optimizer trajectory. To accomplish this, we invoke the K -function of Ripley [53], a commonly used spatial statistic to determine spatial inhomogeneity. For a point process N on \mathbb{R}^D , the K -function is defined for each $r > 0$ as the ratio of the expected number of points within distance r of any randomly chosen point, and the average density of points. Letting $W = \{w_1, \dots, w_n\}$ denote a realization of a point process, its K -function can be estimated consistently by [15, eqn. 8.2.18]:

$$\hat{K}(r) = \frac{\text{diam}(W)}{n} \sum_{\substack{i, j=1 \\ i \neq j}}^n \mathbb{1}\{\|w_i - w_j\| \leq r\}, \quad r > 0. \quad (10)$$

The K -function of a homogeneous Poisson process on \mathbb{R}^D with constant intensity λ is given by $K(r) = \pi^{D/2} r^D / \Gamma(1 + \frac{D}{2})$ for $r > 0$ [15, eqn. 8.3.34]. Note that this function is independent of the intensity. Therefore, deviations in the K -function from an $\mathcal{O}(r^D)$ growth rate suggest spatial inhomogeneity, and therefore points which exhibit spatial clustering. Treating an optimizer trajectory W_1, \dots, W_n as the realization of a point process, we can interpret the K -function through (10) and measure spatial clustering of the trajectory. Following the assumptions in Corollary 2 which define α , we can assume that $\|W_i - W_j\| \leq r$ with probability approximately $c_{|i-j|} r^\alpha$ for $0 < r < r_0$, where c_1, \dots, c_n are positive constants. Under this assumption, $\hat{K}(r) \approx C \text{diam}(W) r^\alpha$ for $0 < r < r_0$ and some constant $C > 0$. Therefore, we would expect $\alpha \ll D$ to be an indication that the optimization exhibits significant spatial clustering. By Corollary 2,

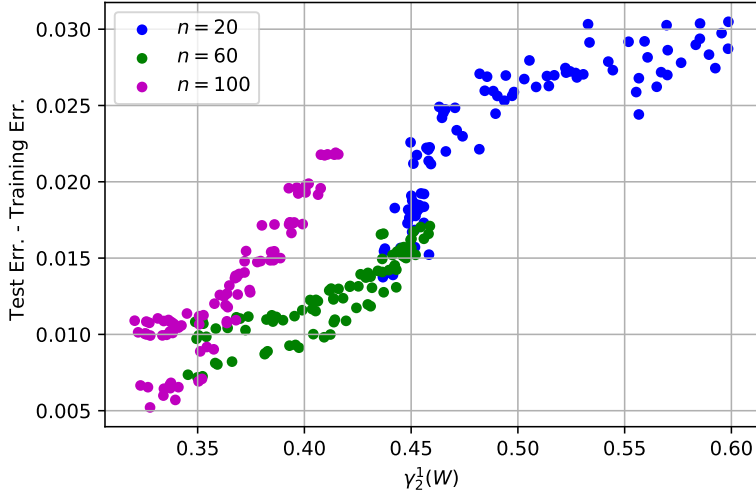


Figure 2: Normalized Fernique–Talagrand functional $\gamma_2^1(W)$ versus generalization gap. Different colors denote different batch-sizes.

this circumstance should coincide with a smaller Fernique–Talagrand functional, and therefore improved generalization.

4 Empirical results

4.1 Direct estimation of the Fernique–Talagrand functional

An attractive feature of the FT functional is the availability of a low-degree polynomial time approximation algorithm for $\gamma_2(W, d)$ when W is a finite subset of \mathbb{R}^D . In particular, [8] shows that $\gamma_2(W, d)$ is computable to ϵ -accuracy in $\mathcal{O}((|W|^{1+\omega} + D|W|^3) \log(|W|D/\epsilon))$ time, and $\omega \leq 2.373$ is the matrix multiplication exponent. To our knowledge, this functional is the only object which tightly bounds (1), up to constants, and is approximable in polynomial time. This is especially attractive for our purposes, providing an effective measure of generalization performance and exploratory capacity, which does *not* require access to any test data. A general procedure to estimate $\gamma_2(W, d)$ is presented in Algorithm 1. To perform the optimization in the final step, any off-the-shelf nonlinear optimization procedure will suffice, including gradient descent. Indeed, since the objective $I_W(p)$ happens to be convex in p (see [8]), any local minimizer p^* with subgradient $\partial I_W(p^*) = 0$ will satisfy $\gamma_2(W, d) = I_W(p^*)$.

Algorithm 1 Fernique–Talagrand functional

Input: A set $W = \{w_1, \dots, w_n\}$, and metric $d(w, w')$ on W

Output: An estimate of $\gamma_2(W, d)$.

- 1: Compute Gram matrix $G = (d(w_i, w_j))_{i,j=1}^n$
 - 2: **for** $i = 1, \dots, n$
 - 3: sort $(G_{ij})_{j=1}^n$ in ascending order to obtain $(\tilde{G}_{ij})_{j=1}^n$ and sorted indices $(\iota_{ij})_{j=1}^n$
 - 4: **end for**
 - 5: **function** $I_W(p)$
 - 6: **for** $i = 1, \dots, n$
 - 7: $I_W^i(p) = \sum_{j=0}^{n-1} \tilde{G}_{ij} \sqrt{|\log \sum_{k=0}^j p_{\iota_{ik}}|}$
 - 8: **return** $\max\{I_W^1(p), \dots, I_W^n(p)\}$
 - 9: **end function**
 - 10: **return** $\min_{z \in \mathbb{R}^n} I_W(\text{softmax}(z))$
-

Unfortunately, this approach becomes more challenging in high dimensions, where the optimization task becomes more difficult to solve to reasonable accuracy. Hence, we restrict our discussion in this section to smaller models. Our model of choice is a three-layer fully-connected neural network with 20 hidden units, applied to the least-squares regression task on the Wine Quality UCI dataset [14]. Models are trained from the same (random) initialization for 30 epochs (*before* convergence) using SGD with constant step size $\eta \in \{0.01, 0.005, 0.001\}$, batch size $b \in \{20, 50, 100\}$, weight decay parameter $\lambda \in [10^{-4}, 5 \times 10^{-4}, 10^{-3}]$, and added zero-mean Gaussian noise to the input data with variance σ^2 for $\sigma \in \{0, 0.05, 0.1\}$. In Figure 2, for each model, we plot generalization error at the end of training against the estimated normalized FT functional (using Algorithm 1) from the last 50 iterates of training. The most profound difference in trends is seen with varying batch size. Nevertheless, as expected, the FT functional shows a strong correlation to generalization error.

4.2 Estimation of the power-law exponents of the transition kernel

Turning our attention to larger models, for the reasons stated in the previous section, here we instead consider the exponent α introduced in Corollary 2, and we develop an efficient method for estimating α . We consider three architectures and two standard image classification datasets. In particular, we consider (i) a fully connected model with 5 layers (FCN5), (ii) a fully connected model with 7 layers (FCN7), and (iii) a convolutional model with 9 layers (CNN9); and two datasets (i) MNIST and (ii) CIFAR10. All models use the ReLU activation function and all are trained with constant step-size SGD, without weight-decay or momentum. Our code is implemented in PyTorch and executed on 5 GeForce GTX 1080 GPUs. For each architecture, we trained the networks with different step-sizes and batch-sizes, where we varied the step-size in the range $[0.002, 0.35]$ and the batch-size in the set $\{50, 100\}$. We trained all models until convergence (i.e., the training accuracy reaches exactly 100%). For measuring the training and test accuracies, we use the standard training-test splits.

To estimate α , once training has converged, we further run the algorithm for $m = 200$ additional iterations to obtain a trajectory $\{W_k\}_{k=1}^m$. Following Corollary 2, we assume *local homogeneity*, that is, the trajectory $\{W_k\}_{k=1}^m$ remains near a local minimum and each $W_{k+1} - W_k$ is approximately iid. Under this assumption, the second term in (8) can be ignored, hence, we compute the sequence $1/\|W_{k+1} - W_k\|$ for $k = 1, \dots, m-1$, and then fit a power-law distribution to this one dimensional set of observations. To do this, we use the publicly available `powerlaw` toolbox in Python [13]. Figure 3 visualizes the results. In all configurations, we observe that the results are in accordance with our theory: the estimated power-law exponents α and the

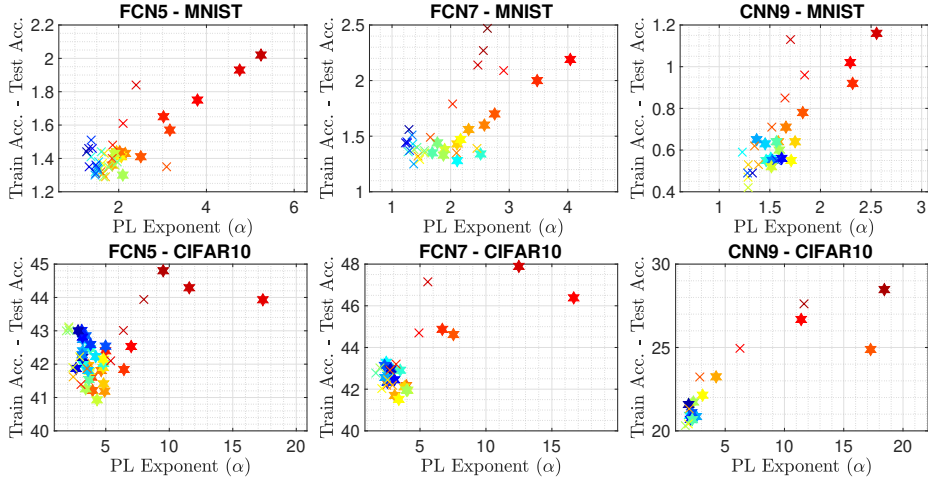


Figure 3: Power-law exponents versus generalization gap. Different colors represent different step-sizes and different markers represent different batch-sizes.

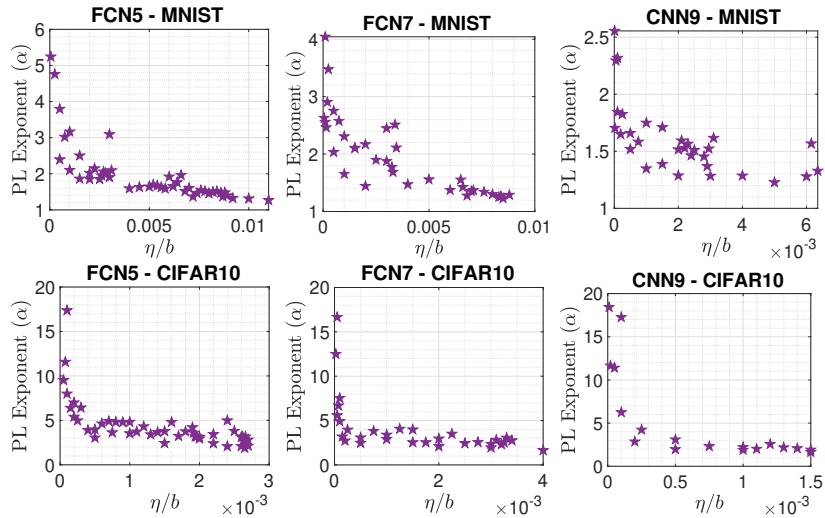


Figure 4: Power-law exponents versus step-size/batch-size ratio (η/b).

generalization gap exhibit significant correlations. We further observe that this trend becomes clearer for the CNN9 model, which might suggest that the geometry induced by the convolutional architecture results in a transition kernel for which the local homogeneity condition becomes more accurate, i.e., the TV term in Corollary 2 becomes smaller.

It has been empirically demonstrated that the generalization performance can depend on the ratio of the step-size to the batch-size η/b [30]. In our final experiments, we monitor the behavior of the power-law exponent α with respect to the SGD hyperparameters: step-size and batch-size. Figure 4 shows the results. We observe that the local power-law behavior of SGD near the found local minimum also heavily depends on the ratio η/b , where we observe a clear monotonicity. This reveals an interesting behavior that the hyperparameters η and b modify the local power-law exponent of the transition kernel, hence the effective dimension, which in turn determines the generalization error. This outcome also shows interesting similarities with the recent studies [25, 28] that has shown that in online SGD (one pass regime with infinite data) the ratio η/b determines the “heaviness of the tails” of the stationary distribution of SGD. Figure 4 suggests that in the finite training data setting (where [25, 28] are not applicable),

another type of power-law behavior is still observed in the local exponent α , which also shows monotonic behavior with respect to η/b . We suspect that this monotonic behavior can be formally quantified, but we leave this as future work.

We finally note that estimating power-law exponents accurately is a challenging task. In particular, for our estimator, it is known that much larger fitted α values, e.g., greater than ca. 5, are less reliable. However, since our empirical results involve running the same experiment multiple times for different hyperparameters that are fairly close to each other, the consistency and the clear trends in our results support our theoretical contributions, even if the estimations are to be inexact.

5 Conclusion

In this paper, we developed a theoretical framework for analyzing the generalization properties of stochastic optimizers by using their trajectories. We first proved generalization bounds based on the celebrated Fernique–Talagrand functional; and then, by using the Markovian structure of stochastic optimizers, we specialized these results to Markov processes. Our results indicates that, in the case when the training algorithm forms a Markov process, the generalization error can be linked to the structure of the corresponding Markov transition kernel. Furthermore, when the Markov kernel can be locally approximated by a power-law distribution, the power-law exponent acts as an effective dimension and has a direct impact on the generalization error. Finally, we supported our theory with empirical results on several simple neural network models.

Acknowledgments. We would like to acknowledge DARPA, NSF, and ONR for providing partial support of this work. U.Ş.’s research is supported by the French government under management of Agence Nationale de la Recherche as part of the “Investissements d’avenir” program, reference ANR-19-P3IA-0001 (PRAIRIE 3IA Institute).

References

- [1] A. Antos, B. Kégl, T. Linder, and G. Lugosi. Data-dependent margin-based generalization bounds for classification. *Journal of Machine Learning Research*, 3(Jul):73–98, 2002.
- [2] S. Arora, N. Cohen, W. Hu, and Y. Luo. Implicit regularization in deep matrix factorization. In *Advances in Neural Information Processing Systems*, volume 32. Curran Associates, Inc., 2019.
- [3] S. Arora, R. Ge, B. Neyshabur, and Y. Zhang. Stronger generalization bounds for deep nets via a compression approach. In *International Conference on Machine Learning*, pages 254–263. PMLR, 2018.
- [4] A. R. Asadi, E. Abbe, and S. Verdú. Chaining mutual information and tightening generalization bounds. *arXiv preprint [arXiv:1806.03803](https://arxiv.org/abs/1806.03803)*, 2018.
- [5] J.-Y. Audibert and O. Bousquet. Combining PAC-Bayesian and generic chaining bounds. *Journal of Machine Learning Research*, 8(Apr):863–889, 2007.
- [6] P. Bartlett, D. J. Foster, and M. Telgarsky. Spectrally-normalized margin bounds for neural networks. *arXiv preprint [arXiv:1706.08498](https://arxiv.org/abs/1706.08498)*, 2017.
- [7] P. L. Bartlett and P. M. Long. Failures of model-dependent generalization bounds for least-norm interpolation. *arXiv preprint [arXiv:2010.08479](https://arxiv.org/abs/2010.08479)*, 2020.

- [8] S. Borst, D. Dadush, N. Olver, and M. Sinha. Majorizing measures for the optimizer. *arXiv preprint arXiv:2012.13306*, 2020.
- [9] S. Boucheron, G. Lugosi, and P. Massart. *Concentration inequalities: A nonasymptotic theory of independence*. Oxford university press, 2013.
- [10] Y. Bu, S. Zou, and V. V. Veeravalli. Tightening mutual information-based bounds on generalization error. *IEEE Journal on Selected Areas in Information Theory*, 1(1):121–130, 2020.
- [11] Y. Cao and Q. Gu. Generalization error bounds of gradient descent for learning over-parameterized deep ReLU networks. *Proceedings of the AAAI Conference on Artificial Intelligence*, 34(04):3349–3356, Apr. 2020.
- [12] L. Chizat, E. Oyallon, and F. Bach. On lazy training in differentiable programming. *arXiv preprint arXiv:1812.07956*, 2018.
- [13] A. Clauset, C. R. Shalizi, and M. E. Newman. Power-law distributions in empirical data. *SIAM review*, 51(4):661–703, 2009.
- [14] P. Cortez, A. Cerdeira, F. Almeida, T. Matos, and J. Reis. Modeling wine preferences by data mining from physicochemical properties. *Decision support systems*, 47(4):547–553, 2009.
- [15] N. Cressie. *Statistics for spatial data*. John Wiley & Sons, 2015.
- [16] A. Dieuleveut, A. Durmus, and F. Bach. Bridging the gap between constant step size stochastic gradient descent and Markov chains. *arXiv preprint arXiv:1707.06386*, 2017.
- [17] L. Dinh, R. Pascanu, S. Bengio, and Y. Bengio. Sharp minima can generalize for deep nets. In *International Conference on Machine Learning*, pages 1019–1028. PMLR, 2017.
- [18] R. M. Dudley. The sizes of compact subsets of Hilbert space and continuity of Gaussian processes. *Journal of Functional Analysis*, 1(3):290–330, 1967.
- [19] F. Farnia, J. Zhang, and D. Tse. A spectral approach to generalization and optimization in neural networks, 2018.
- [20] H. Federer. *Geometric measure theory*. Springer, 2014.
- [21] X. Fernique. Régularité de processus gaussiens. *Inventiones Mathematicae*, 12(4):304–320, 1971.
- [22] X. Fernique. Régularité des trajectoires des fonctions aléatoires gaussiennes. In *Ecole d’Eté de Probabilités de Saint-Flour IV—1974*, pages 1–96. Springer, 1975.
- [23] X. Fontaine, V. De Bortoli, and A. Durmus. Continuous and discrete-time analysis of stochastic gradient descent for convex and non-convex functions. *arXiv preprint arXiv:2004.04193*, 2020.
- [24] S. Fort, G. K. Dziugaite, M. Paul, S. Kharaghani, D. M. Roy, and S. Ganguli. Deep learning versus kernel learning: an empirical study of loss landscape geometry and the time evolution of the Neural Tangent Kernel. *arXiv preprint arXiv:2010.15110*, 2020.
- [25] M. Gurbuzbalaban, U. Simsekli, and L. Zhu. The heavy-tail phenomenon in SGD. *arXiv preprint arXiv:2006.04740*, 2020.

- [26] M. Haghifam, J. Negrea, A. Khisti, D. M. Roy, and G. K. Dziugaite. Sharpened generalization bounds based on conditional mutual information and an application to noisy, iterative algorithms. *arXiv preprint [arXiv:2004.12983](https://arxiv.org/abs/2004.12983)*, 2020.
- [27] M. Hardt, B. Recht, and Y. Singer. Train faster, generalize better: Stability of stochastic gradient descent. In M. F. Balcan and K. Q. Weinberger, editors, *Proceedings of The 33rd International Conference on Machine Learning*, volume 48 of *Proceedings of Machine Learning Research*, pages 1225–1234, New York, New York, USA, 20–22 Jun 2016. PMLR.
- [28] L. Hodgkinson and M. W. Mahoney. Multiplicative noise and heavy tails in stochastic optimization. *arXiv preprint [arXiv:2006.06293](https://arxiv.org/abs/2006.06293)*, 2020.
- [29] S. Jastrzebski, D. Arpit, O. Astrand, G. B. Kerg, H. Wang, C. Xiong, R. Socher, K. Cho, and K. J. Geras. Catastrophic fisher explosion: Early phase Fisher matrix impacts generalization. In *International Conference on Machine Learning*, pages 4772–4784, 2021.
- [30] S. Jastrzebski, Z. Kenton, D. Arpit, N. Ballas, A. Fischer, Y. Bengio, and A. Storkey. Three factors influencing minima in SGD. In *Artificial Neural Networks and Machine Learning*, 2018.
- [31] S. Jastrzebski, M. Szymczak, S. Fort, D. Arpit, J. Tabor, K. Cho, and K. Geras. The Break-Even Point on Optimization Trajectories of Deep Neural Networks. In *International Conference on Learning Representations*, 2020.
- [32] Y. Jiang, B. Neyshabur, H. Mobahi, D. Krishnan, and S. Bengio. Fantastic generalization measures and where to find them. *arXiv preprint [arXiv:1912.02178](https://arxiv.org/abs/1912.02178)*, 2019.
- [33] N. S. Keskar, D. Mudigere, J. Nocedal, M. Smelyanskiy, and P. T. P. Tang. On large-batch training for deep learning: Generalization gap and sharp minima. *arXiv preprint [arXiv:1609.04836](https://arxiv.org/abs/1609.04836)*, 2016.
- [34] A. Lewkowycz, Y. Bahri, E. Dyer, J. Sohl-Dickstein, and G. Gur-Ari. The large learning rate phase of deep learning: the catapult mechanism. *arXiv preprint [arXiv:2003.02218](https://arxiv.org/abs/2003.02218)*, 2020.
- [35] J. Li, X. Luo, and M. Qiao. On generalization error bounds of noisy gradient methods for non-convex learning. *arXiv preprint [arXiv:1902.00621](https://arxiv.org/abs/1902.00621)*, 2019.
- [36] Y. Li, C. Wei, and T. Ma. Towards explaining the regularization effect of initial large learning rate in training neural networks. *arXiv preprint [arXiv:1907.04595](https://arxiv.org/abs/1907.04595)*, 2019.
- [37] L. Liu and Y. Xiao. Hausdorff dimension theorems for self-similar Markov processes. *Probability and Mathematical Statistics*, 18, 1998.
- [38] S. Mandt, M. Hoffman, and D. Blei. A variational analysis of stochastic gradient algorithms. In *International conference on machine learning*, pages 354–363. PMLR, 2016.
- [39] C. H. Martin and M. W. Mahoney. Rethinking generalization requires revisiting old ideas: statistical mechanics approaches and complex learning behavior. *arXiv preprint [arXiv:1710.09553](https://arxiv.org/abs/1710.09553)*, 2017.
- [40] C. H. Martin and M. W. Mahoney. Traditional and heavy-tailed self regularization in neural network models. *Proceedings of the 36th International Conference on Machine Learning (ICML 2019)*, 2019.

- [41] C. H. Martin and M. W. Mahoney. Heavy-tailed Universality predicts trends in test accuracies for very large pre-trained deep neural networks. In *Proceedings of the 2020 SIAM International Conference on Data Mining*, pages 505–513. SIAM, 2020.
- [42] C. H. Martin and M. W. Mahoney. Implicit self-regularization in deep neural networks: Evidence from random matrix theory and implications for learning. *Journal of Machine Learning Research*, 2021.
- [43] C. H. Martin and M. W. Mahoney. Post-mortem on a deep learning contest: a Simpson’s paradox and the complementary roles of scale metrics versus shape metrics. *arXiv preprint arXiv:2106.00734*, 2021.
- [44] C. H. Martin, T. S. Peng, and M. W. Mahoney. Predicting trends in the quality of state-of-the-art neural networks without access to training or testing data. *Nature Communications*, 12(1):1–13, 2021.
- [45] P. Mattila. *Geometry of sets and measures in Euclidean spaces: fractals and rectifiability*. Number 44. Cambridge University Press, 1999.
- [46] M. Mohammadi, A. Mohammadpour, and H. Ogata. On estimating the tail index and the spectral measure of multivariate α -stable distributions. *Metrika*, 78(5):549–561, 2015.
- [47] W. Mou, L. Wang, X. Zhai, and K. Zheng. Generalization bounds of SGLD for non-convex learning: Two theoretical viewpoints. In *Conference on Learning Theory*, pages 605–638. PMLR, 2018.
- [48] J. Negrea, M. Haghifam, G. K. Dziugaite, A. Khisti, and D. M. Roy. Information-theoretic generalization bounds for SGLD via data-dependent estimates. *arXiv preprint arXiv:1911.02151*, 2019.
- [49] B. Neyshabur, S. Bhojanapalli, D. McAllester, and N. Srebro. Exploring generalization in deep learning. In *Advances in Neural Information Processing Systems*, pages 5947–5956, 2017.
- [50] A. Orvieto and A. Lucchi. Continuous-time models for stochastic optimization algorithms. *arXiv preprint arXiv:1810.02565*, 2018.
- [51] A. Panigrahi, R. Somani, N. Goyal, and P. Netrapalli. Non-gaussianity of stochastic gradient noise. *arXiv preprint arXiv:1910.09626*, 2019.
- [52] A. Pensia, V. Jog, and P.-L. Loh. Generalization error bounds for noisy, iterative algorithms. In *2018 IEEE International Symposium on Information Theory (ISIT)*, pages 546–550. IEEE, 2018.
- [53] B. D. Ripley. The second-order analysis of stationary point processes. *Journal of Applied Probability*, 13(2):255–266, 1976.
- [54] D. Russo and J. Zou. How much does your data exploration overfit? Controlling bias via information usage. *IEEE Transactions on Information Theory*, 66(1):302–323, 2019.
- [55] R. L. Schilling. Feller processes generated by pseudo-differential operators: On the hausdorff dimension of their sample paths. *Journal of Theoretical Probability*, 11(2):303–330, 1998.
- [56] S.-J. Sheu. Some estimates of the transition density of a nondegenerate diffusion Markov process. *The Annals of Probability*, pages 538–561, 1991.

- [57] U. Simsekli, M. Gürbüzbalaban, T. H. Nguyen, G. Richard, and L. Sagun. On the heavy-tailed theory of stochastic gradient descent for deep neural networks. *arXiv preprint arXiv:1912.00018*, 2019.
- [58] U. Simsekli, L. Sagun, and M. Gurbuzbalaban. A tail-index analysis of stochastic gradient noise in deep neural networks. In *International Conference on Machine Learning*, pages 5827–5837. PMLR, 2019.
- [59] U. Şimşekli, O. Sener, G. Deligiannidis, and M. A. Erdogdu. Hausdorff Dimension, Stochastic Differential Equations, and Generalization in Neural Networks. *arXiv preprint arXiv:2006.09313*, 2020.
- [60] J. Sokolić, R. Giryes, G. Sapiro, and M. R. Rodrigues. Generalization error of deep neural networks: Role of classification margin and data structure. In *2017 International Conference on Sampling Theory and Applications (SampTA)*, pages 147–151. IEEE, 2017.
- [61] M. Talagrand. Majorizing measures: the generic chaining. *Annals of Probability*, 24(3):1049–1103, 1996.
- [62] M. Talagrand. Majorizing measures without measures. *Annals of Probability*, pages 411–417, 2001.
- [63] M. Talagrand. *Upper and lower bounds for stochastic processes: modern methods and classical problems*, volume 60. Springer Science & Business Media, 2014.
- [64] V. N. Vapnik and A. Y. Chervonenkis. On the uniform convergence of relative frequencies of events to their probabilities. In *Measures of complexity*, pages 11–30. Springer, 2015.
- [65] Y. Xiao. Random fractals and markov processes. *Mathematics Preprint Archive*, 2003(6):830–907, 2003.
- [66] C. Xing, D. Arpit, C. Tsirigotis, and Y. Bengio. A walk with SGD. *arXiv preprint arXiv:1802.08770*, 2018.
- [67] A. Xu and M. Raginsky. Information-theoretic analysis of generalization capability of learning algorithms. *arXiv preprint arXiv:1705.07809*, 2017.
- [68] Y. Yang, L. Hodgkinson, R. Theisen, J. Zou, J. E. Gonzalez, K. Ramchandran, and M. W. Mahoney. Taxonomizing local versus global structure in neural network loss landscapes. *arXiv preprint arXiv:2107.11228*, 2021.
- [69] C. Zhang, S. Bengio, M. Hardt, B. Recht, and O. Vinyals. Understanding deep learning (still) requires rethinking generalization. *Communications of the ACM*, 64(3):107–115, 2021.

A Hausdorff dimension

Here, we shall review facts about the Hausdorff dimension. The Hausdorff measure \mathcal{H}^m on \mathbb{R}^d is defined on a set $E \subseteq \mathbb{R}^d$ by

$$\mathcal{H}^m(E) = \lim_{\delta \rightarrow 0^+} \inf_{\substack{E \subseteq \bigcup_j S_j \\ \text{diam}(S_j) \leq \delta}} \sum_j \alpha(m) 2^{-m} \text{diam}(S_j)^m,$$

where the infimum is taken over countable covers S_δ of E by non-empty subsets of \mathbb{R}^d with diameter not exceeding δ , and $\alpha(m) = \frac{\pi^{n/2}}{\Gamma(n/2+1)}$ is the volume of the unit m -sphere. The following facts are fundamental [20, §2.10.2, §2.10.35]

: (1) if $\mathcal{H}^m(E) < \infty$, then $\mathcal{H}^l(E) = 0$ for any $l > m$; and (2) on \mathbb{R}^d , $\mathcal{H}^d \equiv \mathcal{L}^d$ the d -dimensional Lebesgue measure.

The first fact implies the existence of the *Hausdorff dimension*, which is defined for a set $E \subseteq \mathbb{R}^d$ by $\dim_{\text{H}}(E) = \inf\{m : \mathcal{H}^m(E) = 0\}$. The second fact implies that any set $E \subset \mathbb{R}^d$ with $\dim_{\text{H}}(E) < d$ has zero Lebesgue measure; but, importantly, the converse is not true. In differential geometry, the Hausdorff dimension is useful for identifying the dimension of submanifolds. However, it is also of significant value in the study of fractal sets, providing a measurement of “clustering” in space. One can intuit this from the definition, but it is perhaps best seen through examples. In Figure 1, a Lévy process with sample paths possessing Hausdorff dimension 1.5 is compared to Brownian motion, whose sample paths have Hausdorff dimension 2. The Lévy process, with the smaller Hausdorff dimension, exhibits dynamics with tighter clusters separated by large jumps.

B Growth exponent as intrinsic dimension

Here, we shall discuss the relationship between the exponent α and the dimension D . The most commonly considered discrete-time model for a stochastic optimizer is the perturbed gradient descent (GD) model, which satisfies $W_{k+1} = W_k - \gamma(\nabla f(W_k) + Z_k)$, where Z_k is a Gaussian random vector with zero mean and constant covariance matrix Σ . In the neighborhood of a local minimum w^* , $\nabla f(W_k) \approx 0$, and hence the perturbed gradient descent model resembles a Gaussian random walk $W_{k+1} = W_k + \gamma Z_k$. In this case, if D denotes the ambient dimension, the k -step transition kernel becomes that of a D -dimensional multivariate normal distribution with covariance matrix $k\Sigma$:

$$P^k(x, E) = (2\pi k)^{-\frac{D}{2}} |\det \Sigma|^{-\frac{1}{2}} \int_E \exp\left(-\frac{1}{2k}(y-x)^\top \Sigma^{-1}(y-x)\right) dy.$$

Since Σ is necessarily positive-definite, letting σ_1 and σ_D denote the largest and smallest singular values of Σ respectively, for any $x \in \mathbb{R}^D$ and set $E \subset \mathbb{R}^D$,

$$\frac{1}{(2\pi k\sigma_1)^{D/2}} \int_E \exp\left(-\frac{\|y-x\|^2}{2k\sigma_D}\right) dy \leq P^k(x, E) \leq \frac{1}{(2\pi k\sigma_D)^{D/2}} \int_E \exp\left(-\frac{\|y-x\|^2}{2k\sigma_1}\right) dy. \quad (11)$$

Applying Lemma 4 to (11), we see that for the perturbed GD model, α in Corollary 2 is precisely the ambient dimension D .

C Correlations between types of power-law exponents

Here, we shall discuss the relationship between the power-law exponent in Corollary 2 and the tail exponent seen in [25, 28, 57, 59]. In the general case, *a priori*, there is no reason to expect the two exponents to correlate. Indeed, consider the beta-prime distribution

$$p(x) = \frac{x^{\alpha-1}(1+x)^{-\alpha-\beta}}{B(\alpha, \beta)}, \quad \text{for } x > 0, \quad (12)$$

where $B(\alpha, \beta)$ is the beta function, and $\alpha, \beta > 0$. Symmetrizing this distribution, we find that the Markov chain $W_{k+1} = W_k + \epsilon_k B_k$ where B_k is iid with density (12) and ϵ_k is

Rademacher-distributed has transition kernel $P(x, E)$ satisfying $P(x, B_r(x)) \sim cr^\alpha$ as $r \rightarrow 0^+$ and $P(x, B_r(x)) \sim cr^{-\alpha-\beta+1}$ as $r \rightarrow \infty$. In this case, the power-law exponent in Corollary 2 is α , while the tail exponent in [57] is $\alpha + \beta - 1$, differing according to the parameter β , which may be chosen arbitrarily.

In practice, however, we expect the two to be somewhat correlated, and we justify this through the model considered in [57]. Building on the classical perturbed GD model, the Gaussian updates are replaced by *heavy-tailed* α -stable distributed random variables, justified through the generalized central limit theorem. In this case, the model satisfies

$$W_{k+1} = W_k - \eta(\nabla f(W_k) + S_k(W_k)),$$

where $S_k(w) = (S_k^i(w))_{i=1}^n$ and each $S_k^i(w)$ is independent symmetric α -stable with scale $\sigma(w)$, that is, $S_k^i(w)$ has characteristic function $\varphi(t) = e^{-|\sigma(w)t|^\alpha}$. As $\eta \rightarrow 0^+$, this Markov chain behaves similarly to the stochastic differential equation

$$dW_t = -\nabla f(W_t)dt + \eta^{\frac{\alpha-1}{\alpha}} \sigma dL_t^\alpha, \quad (13)$$

where L_t^α is an α -stable Lévy process (see [57] for details). If ∇f is bounded, the process satisfies the following two properties:

$$\int_0^1 P_t(x, B_r(x))dt \sim c_1 r^\alpha \quad \text{as } r \rightarrow 0^+; \quad \int_0^1 P_t(x, B_r(x))dt \sim c_2 r^{-\alpha} \quad \text{as } r \rightarrow \infty.$$

Therefore, both the power-law exponent in Corollary 2 and the tail exponent in [57] are identical in this model. Empirically, we find that while the two exponents are not identical, they do appear to correlate.

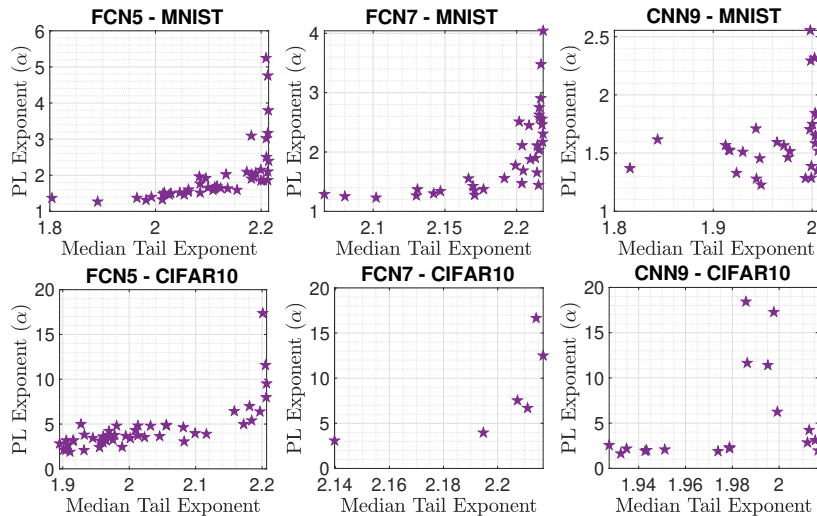


Figure 5: Power-law exponents versus the tail-exponent estimates used in [25].

In Figure 5 we illustrate this relationship. We follow the setup of [25] and assume that each layer of the neural network possesses a different tail-exponent, where these layer-wise tail-exponents are computed on averaged iterates under the assumption that they are distributed from an α -stable distribution. We use the same tail-exponent estimator [46] as the one used in [25]. Once the layer-wise indices are computed, we compute the median tail-exponent over the layers. As we can observe from Figure 5, our power-law exponent and the tail-exponent estimate show a strong correlation. We leave a more detailed analysis of this relationship as future work.

D Proofs of our main results

D.1 Proof of Theorem 1 and Corollary 1

The total mutual information is valuable as it precisely defines the degree to which we may decouple two random elements, as shown in the following lemma.

Lemma 1. *For any Borel set B , $\mathbb{P}_{X,Y}(B) \leq \exp I_\infty(X, Y) \cdot \mathbb{P}_X \otimes \mathbb{P}_Y(B)$.*

Proof. The proof relies on the data processing inequality for α -Renyi divergence, which implies that for any $\alpha > 1$:

$$D_\alpha(\mathbb{B}(\mathbb{P}_{X,Y}(B)) \parallel \mathbb{B}(\mathbb{P}_X \otimes \mathbb{P}_Y(B))) \leq I_\alpha(X, Y),$$

where $\mathbb{B}(p)$ is a Bernoulli measure with success probability p . Therefore, letting $p = \mathbb{P}_{X,Y}(B)$ and $q = \mathbb{P}_X \otimes \mathbb{P}_Y(B)$, as $\alpha \rightarrow \infty$,

$$\begin{aligned} D_\alpha(\mathbb{B}(p) \parallel \mathbb{B}(q)) &= \frac{1}{\alpha - 1} \log \left(q \frac{p^\alpha}{q^\alpha} + (1 - q) \frac{(1 - p)^\alpha}{(1 - q)^\alpha} \right) \\ &= \log \left(\left(q \frac{p^\alpha}{q^\alpha} + (1 - q) \frac{(1 - p)^\alpha}{(1 - q)^\alpha} \right)^{1/(\alpha - 1)} \right) \rightarrow \log \max \left\{ \frac{p}{q}, \frac{1 - p}{1 - q} \right\}. \end{aligned}$$

Therefore, it follows that $p/q \leq \sup_\alpha \exp I_\alpha(X, Y) = \exp I_\infty(X, Y)$. \square

Proof of Theorem 1. In the sequel, we shall let $K > 0$ denote a universal constant, not necessarily the same in each appearance. Let $d_\rho(w, w') = \min\{\rho, \|x - y\|\}$, and consider the alternative *generic chaining* functional $\hat{\gamma}$ given by

$$\hat{\gamma}_2(W, d_\rho) = \inf \sup_{w \in W} \sum_{k=1}^{\infty} 2^{n/2} d_\rho(w, T_k),$$

where the infimum is taken over all sequences of subsets $\{T_k\}_{k=1}^{\infty}$ such that $|T_k| \leq N_k$ (where $N_0 = 1$ and $N_k = 2^{2^k}$ otherwise). By [62, Theorem 1.1], there exists a universal constant $K > 0$ such that $\hat{\gamma}_2(W, d_\rho) \leq K \gamma_2^\rho(W)$. The proof proceeds in a similar fashion to [63, Theorem 2.2.27]. For each k , let T_k^W be a set such that $|T_k^W| \leq N_k$ and

$$\sup_{w \in W} \sum_{k=1}^{\infty} 2^{k/2} d_\rho(w, T_k^W) \leq 2 \hat{\gamma}_2(W, d_\rho).$$

To construct an increasing sequence of subsets, let $U_k^W = \bigcup_{m \leq k} T_m^W$, so that $U_0^W = T_0^W$ and $|U_k^W| \leq 2N_k$. Now, let $Y_w = n^{1/2}[\mathcal{R}_n(w) - \mathcal{R}(w)] / \max\{B/\rho, L\}$, so that $\mathbb{E}Y_w = 0$, and by Hoeffding's inequality, for any $u > 0$ and $w, w' \in \mathbb{R}^D$,

$$\mathbb{P}(|Y_w - Y_{w'}| > u d_\rho(w, w')) \leq 2 \exp(-\frac{1}{2}u^2). \quad (14)$$

For $u > 0$, consider the event $\Omega(u)$ where

$$\forall k \geq 1, \forall w, w' \in U_k^W, |Y_w - Y_{w'}| \leq 2(2^{k/2} + u)d_\rho(w, w').$$

For each k , let \tilde{U}_k^W be an independent copy of U_k^W . Then, for $M = \exp I_\infty(X, W)$,

$$\begin{aligned}
\mathbb{P}(\Omega \setminus \Omega(u)) &\leq \sum_{k=1}^{\infty} \mathbb{E}\mathbb{P}(|Y_w - Y_{w'}| \leq 2(2^{k/2} + u)d_\rho(w, w'), \forall w, w' \in U_k^W \mid U_k^W) \\
&\leq M \sum_{k=1}^{\infty} \mathbb{E}\mathbb{P}(|Y_w - Y_{w'}| \leq 2(2^{k/2} + u)d_\rho(w, w'), \forall w, w' \in \tilde{U}_k^W \mid \tilde{U}_k^W) \\
&\leq M \sum_{k=1}^{\infty} 2^{2(2^k+1)+1} \exp(-2(2^k + u^2)) \\
&\leq M \sum_{k=1}^{\infty} \exp(2(2^k + 1) + 1) \exp(-2(2^k + u^2)) \\
&\leq KM \exp(-2u^2).
\end{aligned}$$

For each element $w \in W$, we define a sequence of (random) integers $k(w, q)$ in the following inductive manner. First, let $k(w, 0) = 0$, and for each $q \geq 1$, we define

$$k(w, q) = \inf \left\{ k : k \geq k(w, q-1), d_\rho(w, U_k^W) \leq \frac{1}{2}d_\rho(w, U_{k(w, q-1)}^W) \right\}.$$

Now, consider elements $\pi_q(w) \in U_{k(w, q)}^W$ satisfying $d_\rho(w, \pi_q(w)) = d_\rho(w, U_{k(w, q)}^W)$. By induction, we find that $d_\rho(w, \pi_q(w)) \leq \rho 2^{-q}$. Furthermore, when $\Omega(u)$ occurs, since $\pi_q(w) \in U_{k(w, q)}^W$ and $\pi_{q-1}(w) \in U_{k(w, q-1)}^W \subset U_{k(w, q)}^W$, it follows that

$$|Y_{\pi_q(w)} - Y_{\pi_{q-1}(w)}| \leq 2(2^{k(w, q)/2} + u)d_\rho(\pi_q(w), \pi_{q-1}(w)).$$

Therefore, letting $w_0 \in T_0^W$, under $\Omega(u)$,

$$\begin{aligned}
|Y_w - Y_{w_0}| &\leq \sum_{q=1}^{\infty} |Y_{\pi_q(w)} - Y_{\pi_{q-1}(w)}| \\
&\leq \sum_{q=1}^{\infty} 2(2^{k(w, q)/2} + u)d_\rho(\pi_q(w), \pi_{q-1}(w)) \\
&\leq \sum_{q=1}^{\infty} 2(2^{k(w, q)/2} + u)d_\rho(w, \pi_q(w)) + \sum_{q=1}^{\infty} 2(2^{k(w, q)/2} + u)d_\rho(w, \pi_{q-1}(w)).
\end{aligned}$$

By construction,

$$\sum_{q=1}^{\infty} 2^{k(w, q)/2} d_\rho(w, \pi_q(w)) \leq \sum_{k=0}^{\infty} 2^{k/2} d_\rho(w, T_n^W) \leq 2\hat{\gamma}_2(W, d_\rho).$$

Similarly, by the definition of $k(w, q)$, it follows that $d_\rho(w, U_{k(w, q)}^W) \leq \frac{1}{2}d_\rho(w, U_{k(w, q-1)}^W)$ and $d_\rho(w, U_{k(w, q-1)}^W) \geq \frac{1}{2}d_\rho(w, U_{k(w, q-1)}^W)$. Therefore,

$$\begin{aligned}
\sum_{q=1}^{\infty} 2^{k(w, q)/2} d_\rho(w, \pi_{q-1}(w)) &\leq 2 \sum_{q=1}^{\infty} 2^{k(w, q)/2} d_\rho(w, T_{k(w, q)-1}^W) \\
&\leq 4 \sum_{k=0}^{\infty} 2^{k/2} d_\rho(w, T_n^W) \\
&\leq 8\hat{\gamma}_2(W, d_\rho).
\end{aligned}$$

Finally, we have that $\sum_{q=1}^{\infty} d_{\rho}(\pi_q(w), w) \leq \rho \sum_{q=1}^{\infty} 2^{-q} = \rho$, and $\sum_{q=1}^{\infty} d_{\rho}(\pi_{q-1}(w), w) \leq 2\rho$. Therefore, when $\Omega(u)$ occurs, for any $w \in W$,

$$|Y_w - Y_{w_0}| \leq K(\hat{\gamma}_2(W, d_{\rho}) + \rho u) \leq K(\gamma_2^{\rho}(W) + \rho u).$$

Altogether, this implies that

$$\mathbb{P}\left(\sup_{w, w' \in W} |Y_w - Y_{w'}| > K(\gamma_2^{\rho}(W) + \rho u)\right) \leq K \exp(I_{\infty}(X, W) - 2u^2).$$

Since $\mathbb{E}Y_w = 0$, $\sup_{w \in W} |Y_w| \leq \sup_{w, w' \in W} |Y_w - Y_{w'}|$, and (5) follows. We would now like to apply [67, Lemma 1] to show (6). To do so, it is necessary to show that $\sup_{w \in \tilde{W}} |\mathcal{R}_n(w) - \mathcal{R}(w)|$ is subgaussian, where \tilde{W} is an independent copy of W . Recall that a random variable X is σ -subgaussian if $\log \mathbb{E} \exp(\lambda(X - \mathbb{E}X)) \leq \lambda^2 \sigma^2 / 2$. First, consider the case where $\tilde{W} = \mathcal{W}$ is a deterministic set of weights, and for brevity, let $\bar{\mathcal{R}}_n(w) = \mathcal{R}_n(w) - \mathcal{R}(w)$. In this case, one may apply McDiarmid's inequality to $\sup_{w \in \mathcal{W}} |\bar{\mathcal{R}}_n(w)| = f(X_1, \dots, X_n)$, where

$$f(x_1, \dots, x_n) = \sup_{w \in \mathcal{W}} \left| \frac{1}{n} \sum_{i=1}^n \ell(x_i, w) - \mathbb{E} \ell(X_i, w) \right|.$$

Since ℓ is bounded, it follows that $|\ell(x_i, w) - \ell(y_i, w)| \leq 2B$ for any x, y and $w \in \mathcal{W}$. Therefore,

$$|f(x_1, \dots, x_{i-1}, x_i, x_{i+1}, \dots, x_n) - f(x_1, \dots, x_{i-1}, x'_i, x_{i+1}, \dots, x_n)| \leq \frac{2B}{n}.$$

Applying McDiarmid's inequality reveals that

$$\mathbb{P}\left(\left|\sup_{w \in \mathcal{W}} |\bar{\mathcal{R}}_n(w)| - \mathbb{E} \sup_{w \in \mathcal{W}} |\bar{\mathcal{R}}_n(w)|\right| > u\right) \leq 2 \exp\left(-\frac{nu^2}{2B^2}\right).$$

Since the bound does not depend on \mathcal{W} , and $\{X_i\}_{i=1}^n, \tilde{W}$ are independent, we can condition on \tilde{W} and apply this bound to find that

$$\mathbb{P}\left(\left|\sup_{w \in \tilde{W}} |\bar{\mathcal{R}}_n(w)| - \mathbb{E} \sup_{w \in \tilde{W}} |\bar{\mathcal{R}}_n(w)|\right| > u\right) \leq 2 \exp\left(-\frac{nu^2}{2B^2}\right),$$

which, by [9, Theorem 2.1], implies that $\sup_{w \in \tilde{W}} |\bar{\mathcal{R}}_n(w)|$ is $(4B/\sqrt{n})$ -subgaussian. Applying [67, Lemma 1],

$$\mathbb{E} \sup_{w \in \tilde{W}} |\mathcal{R}_n(w) - \mathcal{R}(w)| \leq \mathbb{E} \sup_{w \in \tilde{W}} |\bar{\mathcal{R}}_n(w) - \mathcal{R}(w)| + \sqrt{\frac{32B^2 I_1(X, W)}{n}}. \quad (15)$$

Using (14), an application of [61, Proposition 2.4] shows that

$$\mathbb{E} \sup_{w \in \tilde{W}} |Y_w| \leq \mathbb{E} \left[\mathbb{E}_{\tilde{W}} \sup_{w \in \tilde{W}} |Y_w| \right] \leq K \mathbb{E} \gamma_2^{\rho}(\tilde{W}) = K \mathbb{E} \gamma_2^{\rho}(W), \quad (16)$$

where $\mathbb{E}_{\tilde{W}}$ denotes conditional expectation, conditioned on \tilde{W} . The result now follows by combining (15) and (16). \square

Remark 2. Unfortunately, there has been little work on providing good estimates on the universal constant K . To our knowledge, only the original work of Fernique reports constants: from [22, pg. 74], we find that

$$K \leq 30\sqrt{8} \left[\sqrt{2 + \frac{1}{\log 2}} + \frac{e}{2\sqrt{\log 2}} \right] \approx 296,$$

which is likely much larger than necessary.

Proof of Corollary 1. Define a probability measure μ with support on W by $\mu(E) = \mathcal{H}^\alpha(W \cap E) / \mathcal{H}^\alpha(W)$. By assumption, $\mu(B_r(w)) \geq (C_\rho r)^\alpha$ for $0 \leq r < \rho$ and any $w \in W$. Therefore,

$$\gamma_2^\rho(W) \leq \sup_{w \in W} \frac{1}{\rho} \int_0^\rho \sqrt{\log \frac{1}{\mu(B_r(w))}} dr \leq (C_\rho^{-1} \sqrt{\alpha}) \cdot \frac{1}{\rho} \int_0^{\rho C_\rho} \sqrt{\log \frac{1}{r}} dr.$$

Since $\mu(B_r(w)) \leq 1$, it follows that $\rho C_\rho \leq 1$. The result follows upon the observation that $\int_0^1 \sqrt{\log \frac{1}{r}} dr = \frac{\sqrt{\pi}}{2}$. \square

D.2 Proof of Theorem 2

The Dudley bound is related to the Fernique–Talagrand functional through the following lemma, which combines [63, Corollary 2.3.2] with the discussion on [63, pg. 22]. Let $N_r^d(W)$ denote the r -covering number of W , that is, the smallest integer N such that there exists a set of N balls of radius r under the metric d , whose union contains W .

Lemma 2 (Dudley entropy). *There exists a universal constant $K > 0$ such that for any metric d and set W , $\gamma_2(W, d) \leq K \int_0^\infty \sqrt{\log N_r^d(W)} dr$. In particular, $\gamma_2^\rho(W) \leq \frac{K}{\rho} \int_0^\rho \sqrt{\log N_r(W)} dr$.*

If $W \subset \mathbb{R}^D$, the Dudley bound is never off by any more than a factor of $\log(d+1)$ [63, Exercise 2.3.4]. Now, since $x \mapsto \sqrt{\log x}$ is concave on $[1, \infty)$, Jensen’s inequality implies that $\mathbb{E}\sqrt{\log X} \leq \sqrt{\mathbb{E}\log X}$ for any random variable with support in $[1, \infty)$. Therefore,

$$\mathbb{E}\gamma_2^\rho(W) \leq \frac{K}{\rho} \int_0^\rho \sqrt{\log \mathbb{E}N_r(W)} dr.$$

Covering numbers for images of Markov processes are bounded by the following fundamental lemma.

Lemma 3. *Let $\Lambda(r)$ be a fixed collection of cubes of side length r in \mathbb{R}^d such that no ball of radius r can intersect more than K cubes of $\Lambda(r)$.*

1. *Suppose that X_n is a time-homogeneous Markov chain with n -step transition kernel $P^n(x, A)$. For any integer m , let $\mathcal{N}_r(m)$ denote the number of cubes in $\Lambda(r)$ hit by X_n at some time $0 \leq k \leq m$. Then*

$$\mathbb{E}\mathcal{N}_r(m) \leq 2K \left[\inf_{x \in \bigcup_{r>0} \Lambda(r)} \mathbb{E}_x \left(\frac{1}{m} \sum_{k=1}^m P^k(x, B_{r/3}(x)) \right) \right]^{-1}.$$

2. *Suppose that X_t is a time-homogeneous strong Markov process in \mathbb{R}^d with transition kernel $P(t, x, A)$. For any $t \geq 0$, let $\mathcal{N}_r(t)$ denote the number of cubes in $\Lambda(r)$ hit by X_t at some time $s \in [0, t]$. Then*

$$\mathbb{E}\mathcal{N}_r(t) \leq 2K \left[\inf_{x \in \bigcup_{r>0} \Lambda(r)} \mathbb{E}_x \left(\frac{1}{t} \int_0^t P(s, x, B_{r/3}(x)) ds \right) \right]^{-1}.$$

Proof. The second result is precisely [37, Lemma 3.1], so it will suffice to show only the first. In a similar fashion, we consider a sequence of stopping times constructed in the following manner: let $\tau_0 = 0$ and for each positive integer j , we let

$$\tau_j = \min \left\{ k \geq \tau_{j-1} : \min_{i=0, \dots, j-1} |X_k - X_{\tau_i}| > r \right\}.$$

In other words, each τ_j is chosen to be the first time that the Markov chain is at least distance r from $X_{\tau_0}, \dots, X_{\tau_{j-1}}$. By construction, $|X_{\tau_j} - X_{\tau_k}| \geq r$ for $j \neq k$. By a Vitali covering argument, the balls $\{B_{r/3}(X_{\tau_j})\}_j$ are disjoint. Now, let

$$T_j = \sum_{k=\tau_j+1}^{\tau_j+m} \mathbb{1}_{X_k \in B_{r/3}(X_{\tau_j})}$$

be the sojourn time of X_k in $B_{r/3}(X_{\tau_j})$ in the interval $(\tau_j, \tau_j + m]$. Furthermore, let $\eta = \min\{k : \tau_k > m\}$ so that $\{X_k\}_{k=0}^m \subset \bigcup_{j=0}^{\eta-1} B_r(X_{\tau_j})$. Therefore, because $\{X_k\}_{k=0}^m$ is contained within the union of η balls in \mathbb{R}^d and no ball in \mathbb{R}^d can intersect any more than K cubes of $\Lambda(r)$, it follows that

$$\mathcal{N}_r(m) \leq K\eta. \quad (17)$$

Let I_j be the indicator of the event $\{\tau_j \leq m\}$, or equivalently, $\{\eta - 1 \geq j\}$. Doing so, we have that $\eta = \sum_{j=0}^{\infty} I_j$. Furthermore, since $\sum_{j=0}^{\infty} \mathbb{1}_{X_k \in B_{r/3}(X_{\tau_j})} \leq 1$ by the disjointness of $\{B_{r/3}(X_{\tau_j})\}_j$,

$$\begin{aligned} \sum_{j=0}^{\infty} I_j T_j &= \sum_{j=0}^{\infty} \sum_{k=\tau_j+1}^{\tau_j+m} \mathbb{1}_{\tau_j \leq m} \mathbb{1}_{X_k \in B_{r/3}(X_{\tau_j})} \\ &\leq \sum_{k=1}^{2m} \sum_{j=0}^{\infty} \mathbb{1}_{X_k \in B_{r/3}(X_{\tau_j})} = 2m. \end{aligned}$$

By the strong Markov property, we may condition on starting the process at X_{τ_j} :

$$\begin{aligned} \mathbb{E}[I_j T_j] &= \mathbb{E} \left[\mathbb{1}_{\tau_j \leq m} \mathbb{E}_{X_{\tau_j}} \sum_{k=1}^m \mathbb{1}_{X_k \in B_{r/3}(X_{\tau_j})} \right] \\ &\geq \mathbb{E} I_j \cdot \inf_{x \in \mathbb{R}^d} \mathbb{E}_x \sum_{k=1}^m \mathbb{1}_{X_k \in B_{r/3}(x)}. \end{aligned}$$

Therefore, by monotone convergence,

$$\begin{aligned} \mathbb{E} \eta \cdot \inf_{x \in \mathbb{R}^d} \mathbb{E}_x \sum_{k=1}^m \mathbb{1}_{X_k \in B_{r/3}(x)} &= \sum_{j=0}^{\infty} \mathbb{E} I_j \inf_{x \in \mathbb{R}^d} \mathbb{E}_x \sum_{k=1}^m \mathbb{1}_{X_k \in B_{r/3}(x)} \\ &\leq \sum_{j=0}^{\infty} \mathbb{E}[I_j T_j] = \mathbb{E} \sum_{j=0}^{\infty} I_j T_j \leq 2m, \end{aligned}$$

and hence

$$\mathbb{E} \eta \leq 2 \left[\inf_{x \in \mathbb{R}^d} \mathbb{E}_x \left(\frac{1}{m} \sum_{k=1}^m \mathbb{1}_{X_k \in B_{r/3}(x)} \right) \right]^{-1}. \quad (18)$$

The result now follows from (17) and (18). \square

If $\Lambda(r)$ is chosen to be the set of dyadic cubes in \mathbb{R}^D of side length r , then $K = 3^D$. Combining Lemmas 2 and 3 with this choice of $\Lambda(r)$ yields Theorem 2.

D.3 Proof of (9)

The proof of (9) relies on the following simple lemma.

Lemma 4. For any $a > 0$, $x \in \mathbb{R}^D$, and $0 \leq r \leq \rho$,

$$\frac{r^D}{2} I_\rho(a, D) \leq \int_{B_r(x)} e^{-a\|y-x\|^2} dy \leq \frac{r^D}{D},$$

where $I_\rho(a, D) = \int_0^1 v^{D/2-1} e^{-av\rho^2} dv$ is monotone decreasing in a , D , and ρ .

Proof. By a change of variables,

$$\int_{B_r(0)} \exp(-a\|x\|^2) dx = \int_0^r u^{D-1} e^{-au^2} du = \frac{r^D}{2} \int_0^1 v^{D/2-1} e^{-ar^2v} dv.$$

The bounds are obtained through $e^{-av\rho^2} \leq e^{-ar^2v} \leq 1$. \square

Proof of (9). In the sequel, K will be used to denote a universal constant, not necessarily the same at each appearance. First, by the Aronson estimate and Lemma 4,

$$\begin{aligned} \int_0^T P_t(x, B_r(x)) dt &\geq K \int_0^T \int_{B_r(x)} \frac{1}{t^{D/2}} \exp\left(-\frac{\|x-y\|^2}{2\lambda t}\right) dy dt \\ &\geq Kr^D \int_0^T \frac{1}{t^{D/2}} I_\rho\left(\frac{1}{2\lambda t}, D\right) dt. \end{aligned}$$

By Fubini's Theorem, and through the change of variables $t \mapsto t^{-1}$,

$$\begin{aligned} \int_0^T P_t(x, B_r(x)) dt &\geq Kr^D \int_0^1 \int_0^T \frac{1}{t^{D/2}} v^{D/2-1} e^{-v\rho^2/(2\lambda t)} dt dv \\ &\geq Kr^D \int_0^1 \int_{1/T}^\infty s^{D/2-2} v^{D/2-1} e^{-sv\rho^2/2\lambda t} ds dv \\ &\geq KTr^D J_{\rho, T}\left(\frac{1}{2\lambda}, D\right), \end{aligned}$$

where $J_{\rho, T}$ is as defined in Section 3. Equation (9) now follows from Theorem 2. \square

D.4 Proof of Corollary 2

The proof of Corollary 2 itself relies on the following corollary, which performs the local homogeneity approximation to $\{W_k\}_{k=0}^m$.

Corollary 3. Let Ω be a closed set such that $\mathbb{P}(W_k \notin \Omega \text{ for some } k = 0, \dots, m) \leq \zeta_m$. Then for any probability measure μ , letting μ^k denote k -fold convolution of μ and P_Ω the transition kernel of W_k conditioned on $W_k \in \Omega$ for $k = 1, 2, \dots, m$,

$$\begin{aligned} \mathbb{E}\gamma_2^\rho(\{W_k\}_{k=0}^m) &\leq \frac{K}{\rho} \int_0^\rho \sqrt{(D+2) \log 3 - \log\left(\frac{1}{m} \sum_{k=1}^m \mu^k(B_r)\right)} dr \\ &\quad + \sqrt{\log(m+1)} \left(\zeta_m + m \sup_{x \in \Omega} d_{TV}(P_\Omega(x, x + \cdot), \mu) \right). \quad (19) \end{aligned}$$

Proof. Let $\{\bar{W}_k\}_{k=0}^m$ denote the random walk satisfying $\bar{W}_{k+1} = \bar{W}_k + Z_k$, where each $Z_k \sim \mu$ is independent. Since $\gamma_2^\rho(W) \leq \sqrt{\log|W|}$, it follows that

$$\begin{aligned} |\mathbb{E}\gamma_2^\rho(\{W_k\}_{k=0}^m) - \mathbb{E}\gamma_2^\rho(\{\bar{W}_k\}_{k=0}^m)| &\leq \sqrt{\log(m+1)} \sup_{\|f\|_\infty \leq 1} |\mathbb{E}f(\{W_k\}_{k=0}^m) - \mathbb{E}f(\{\bar{W}_k\}_{k=0}^m)| \\ &\leq \sqrt{\log(m+1)} d_{\text{TV}}(\{W_k\}_{k=0}^m, \{\bar{W}_k\}_{k=0}^m). \end{aligned}$$

Since $\mathbb{E}\gamma_2^\rho(\{\bar{W}_k\}_{k=0}^m)$ is bounded above by the first term of (19) by Theorem 2, it suffices to show that

$$d_{\text{TV}}(\{W_k\}_{k=0}^m, \{\bar{W}_k\}_{k=0}^m) \leq \zeta_m + m \sup_{x \in \Omega} d_{\text{TV}}(P_\Omega(x, x + \cdot), \mu).$$

Let Z_k be chosen such that $\{W_k\}_{k=0}^m$ and $\{\bar{W}_k\}_{k=0}^m$ are optimally coupled under the total variation metric, that is,

$$d_{\text{TV}}(\{W_k\}_{k=0}^m, \{\bar{W}_k\}_{k=0}^m) = \mathbb{P}(\{W_k\}_{k=0}^m \neq \{\bar{W}_k\}_{k=0}^m).$$

Conditioning on $W_k \in \Omega$, there is

$$\begin{aligned} d_{\text{TV}}(\{W_k\}_{k=0}^m, \{\bar{W}_k\}_{k=0}^m) &\leq \zeta_m + \mathbb{P}(\{W_k\}_{k=0}^m \neq \{\bar{W}_k\}_{k=0}^m | \{W_k\}_{k=0}^m \in \Omega^m) \\ &\leq \zeta_m + \sum_{j=1}^m \mathbb{P}(W_j \neq \bar{W}_j | \{W_k\}_{k=0}^m \in \Omega^m, \{W_k\}_{k=0}^{j-1} = \{\bar{W}_k\}_{k=0}^{j-1}), \end{aligned}$$

which implies (19). □

Proof of Corollary 2. By the hypotheses, for $\bar{c}_m = m^{-1}(c_1 + \dots + c_m)$, $m^{-1} \sum_{k=1}^m \mu^k(B_r) \geq \bar{c}_m r^\alpha$ for any $0 < r < r_0$. Let $\epsilon > 0$ be arbitrary. Note that if $r \leq \rho_\epsilon := \min\{1, r_0, (\bar{c}_m/3^{D+2})^{1/\epsilon}\}$,

$$\frac{1}{m} \sum_{k=1}^m \mu^k(B_r) \geq 3^{D+2} r^{\alpha+\epsilon}.$$

Therefore, considering the first term on the right hand side of (19), since $\rho_\epsilon \leq 1$,

$$\int_0^{\rho_\epsilon} \sqrt{(D+2) \log 3 - \log \left(\frac{1}{m} \sum_{k=1}^m \mu^k(B_r) \right)} dr \leq \sqrt{\alpha + \epsilon} \int_0^1 \sqrt{\log \frac{1}{r}} dr.$$

The result now follows from Corollary 3. □